https://doi.org/10.5194/egusphere-2023-2666
Preprint. Discussion started: 15 November 2023

Soil carbon-concentration and carbon-climate feedbacks in CMIP6 Earth system models

Rebecca M. Varney[1, 2], Pierre Friedlingstein[1], Sarah E. Chadburn[1], Eleanor J. Burke[3], and Peter M. Cox[1, 2]

[1]Faculty of Environment, Science and Economy, University of Exeter, Laver Building, North Park Road, Exeter, EX4 4QE, UK
[2]Global Systems Institute, University of Exeter, Laver Building, North Park Road, Exeter, EX4 4QE, UK
[3]Met Office Hadley Centre, FitzRoy Road, Exeter, EX1 3PB, UK

Correspondence: Rebecca M. Varney (r.varney@exeter.ac.uk)

Abstract. Achieving climate targets requires mitigation against climate change, but also understanding of the response of land and ocean carbon systems. In this context, global soil carbon stocks and its response to environmental changes is key. This paper quantifies the global soil carbon feedback to changes in atmospheric CO_2, and associated climate changes, for Earth system models (ESMs) in CMIP6. A standard approach is used to calculate carbon cycle feedbacks, defined here as soil specific carbon-concentration (β_s) and carbon-climate (γ_s) feedback parameters. The sensitivity to CO_2 is shown to dominate soil carbon changes at least up to a doubling of atmospheric CO_2. However, the sensitivity of soil carbon to climate change is found to become an increasingly important source of uncertainty under higher atmospheric CO_2 concentrations.

1 Introduction

Global soil carbon stocks contain at least twice as much carbon than is stored in the world's vegetation, making soils the largest active store of carbon on the land surface of Earth (Canadell et al., 2021). In the absence of human disturbance and land-use change, future changes in soil carbon depend on the sensitivity to increases in atmospheric CO_2 concentrations and the sensitivity to the associated impacts of climate change, such as increases to atmospheric temperatures and changes in precipitation patterns (Varney et al., 2023; Todd-Brown et al., 2014). The quantification of such carbon cycle feedbacks is required to determine the overall response of the climate system to given anthropogenic CO_2 emissions and to help achieve Paris Agreement targets (Friedlingstein et al., 2022; Gregory et al., 2009).

Previous studies have defined land carbon cycle feedbacks within Earth system models (ESMs) from both CMIP6 and CMIP5 ensembles (Arora et al., 2020, 2013). In general, the overall response of carbon stores is separated into those due to changes in atmospheric CO_2 (ΔCO_2), and those due to changes in global temperature (ΔT), with the latter assumed to represent the overall impacts of climate change on large spatial scales. These components are called carbon-concentration feedbacks (β_L), and carbon-climate feedbacks (γ_L), respectively (Friedlingstein et al., 2003, 2006). An advantage of using this formulation is that it allows for the quantification of the feedbacks for a given atmospheric CO_2 concentration, which can then be used as a simplified measure to compare amongst ESMs despite the increasing model complexities (Arora et al.,

https://doi.org/10.5194/egusphere-2023-2666
Preprint. Discussion started: 15 November 2023

2020, 2013; Gregory et al., 2009). The technique can be used for both concentration-driven and emission-driven simulations and is a consistent metric to measure land carbon feedbacks despite the differing climate sensitivities amongst ESMs (Boer and Arora, 2013).

In this study, soil carbon driven feedbacks in ESMs are quantified using this $\beta\gamma$ formulation (Friedlingstein et al., 2006). This paper makes use of the latest generation of the Coupled Model Intercomparison Project (CMIP6) used within the Intergovernmental Panel on Climate Change 6$^{\text{th}}$ Assessment Report (IPCC AR6; IPCC (2021); Eyring et al. (2016)). To do this, soil carbon carbon-concentration and carbon-climate feedback parameters are presented, named β_s and γ_s respectively. The aim of this paper is to: (1) quantify the sensitivity of soil carbon to climate change by calculating β_s and γ_s for CMIP6 ESMs; (2) investigate the linearity of future soil carbon change at higher levels of atmospheric CO_2 increase; and (3) identify the fraction of the land surface response to climate change that is due to global soils.

2 Methods

2.1 C4MIP simulations

The Coupled Climate-Carbon Cycle Model Intercomparison Project (C4MIP) was set up to provide a common framework to allow for comparison and consistent evaluation of carbon cycle feedbacks within ESMs (Friedlingstein et al., 2006), and have been used across CMIP generations (Arora et al., 2013, 2020). This framework includes a set of idealised experiments to simplify and quantify the impact of increasing atmospheric CO_2 on the climate system. In these experiments, additional effects such as land-use change, aerosols and non-CO_2 greenhouse gases are not included and nitrogen deposition is fixed at pre-industrial values (Jones et al., 2016).

The control simulation is known as the 1% CO_2 run (CMIP simulation *1pctCO2*), where a consistent 1% increase in atmospheric CO_2 per year is prescribed (referred to in this study as the full 1% CO_2 simulation), starting from pre-industrial concentrations and running for 150 years. Additional experiments were designed to enable the CO_2 and climate effects to be isolated, these are known as: biogeochemically coupled (referred to here as the 'BGC' simulation) and radiatively coupled (referred to here as the 'RAD' simulation) runs. In the BGC runs (CMIP6 simulation *1pctCO2-bgc*), the 1% CO_2 increase per year only affects the carbon cycle component of the ESM while the radiation code continues to see pre-industrial CO_2 values. Conversely, in the RAD runs (CMIP6 simulation *1pctCO2-rad*), the 1% CO_2 increase per year affects only the radiation code, and the carbon cycle component of the ESM continues to see just the pre-industrial CO_2 value (285 ppm).

This study uses the full 1% CO_2, BGC, and RAD C4MIP experiments with ten CMIP6 ESMs (Eyring et al., 2016): ACCESS-ESM1-5, BCC-CSM2-MR, CanESM5, CESM2, GFDL-ESM4, IPSL-CM6A-LR, MIROC-ES2L, MPI-ESM1-2-LR, NorESM2-LM, and UKESM1-0-LL (see Table 1). The ESMs included were chosen due to the availability of the data required at the time of analysis (CMIP6: https://esgf-node.llnl.gov/search/cmip6/, last access: 8 April 2022).

https://doi.org/10.5194/egusphere-2023-2666
Preprint. Discussion started: 15 November 2023

2.2 Defining soil carbon feedbacks

2.2.1 Friedlingstein et al. (2006) $\beta\gamma$ formulation

The standard formulation uses a linear approximation to estimate carbon cycle feedbacks under a changing climate (Friedlingstein et al., 2003, 2006). The change in land carbon storage (ΔC_L, PgC) is approximated linearly using feedback parameters which define separate sensitivities to changes in atmospheric CO_2 (ΔCO_2, ppm) and changes in global temperatures (ΔT, °C), defined as the land carbon-concentration (β_L, PgC ppm^{-1}) and carbon-climate (γ_L, PgC °C^{-1}) (Equation 1).

$$\Delta C_L \approx \beta_L \Delta CO_2 + \gamma_L \Delta T \tag{1}$$

The Friedlingstein et al. (2006) methodology uses time-integrated fluxes (F_L, PgC yr^{-1}), which represent the total change in size of the land carbon pool (ΔC_L). This is presented for the full 1% CO_2 simulation (Equation 2), BGC simulation (Equation 3), and RAD simulation (Equation 4) below, where ΔC_L, ΔC_L^{BGC}, and ΔC_L^{RAD} are the changes in global land carbon pools (PgC), and F_L, F_L^{BGC}, and F_L^{RAD} are the net carbon fluxes to the land (PgC yr^{-1}), for each simulation.

$$\Delta C_L = \int F_L \, dt = \beta_L \Delta CO_2 + \gamma_L \Delta T \tag{2}$$

$$\Delta C_L^{BGC} = \int F_L^{BGC} \, dt = \beta_L \Delta CO_2 + \gamma_L \Delta T^{BGC} \approx \beta_L \Delta CO_2 \tag{3}$$

$$\Delta C_L^{RAD} = \int F_L^{RAD} \, dt = \gamma_L \Delta T^{RAD} \tag{4}$$

In these equations, $\Delta CO_2(t)$ (ppm) is the same in the full 1% CO_2 and BGC simulations (Equations 2 and 3, respectively), as the carbon cycle code sees increased CO_2 in both cases. However, ΔCO_2 can be neglected in Equation 4 as the carbon cycle code sees no increased CO_2 in this case. ΔT, ΔT^{BGC}, and ΔT^{RAD} (°C) are the changes in global temperatures, in the full 1% CO_2, BGC, and RAD simulations, respectively. In Equation 3, ΔT^{BGC} is assumed to be negligible, following Friedlingstein et al. (2006). As the increased CO_2 within the BGC simulation does not affect the radiation code, there is no direct increase in atmospheric temperatures within the model. Arora et al. (2020) explain however, that local changes in the carbon cycle arising from increases in CO_2 affect latent and sensible heat fluxes at the land surface, including: changes to evaporative fluxes from stomatal closure over land and changes in vegetation structure and coverage if dynamic vegetation is included within the ESM (see Table 1). This study assumes that the global temperature changes in the BGC simulation are negligible in the context of the $\beta\gamma$ formulation (Fig. SA1).

https://doi.org/10.5194/egusphere-2023-2666
Preprint. Discussion started: 15 November 2023

2.2.2 Soil carbon-concentration and carbon-climate feedbacks

Global ΔC_L can be written as the sum of the changes in vegetation carbon (ΔC_v) and changes in soil carbon (ΔC_s). Following the $\beta\gamma$ formulation, a similar breakdown of the land carbon-concentration and carbon-climate feedback parameters can be derived, where $\beta_L = \beta_v + \beta_s$ and $\gamma_L = \gamma_v + \gamma_s$ (Equation 5).

$$\Delta C_L \approx (\beta_v + \beta_s)\Delta CO_2 + (\gamma_v + \gamma_s)\Delta T \tag{5}$$

$$\Delta C_v \approx \beta_v \Delta CO_2 + \gamma_v \Delta T \tag{6}$$

$$\Delta C_s \approx \beta_s \Delta CO_2 + \gamma_s \Delta T \tag{7}$$

Therefore, an equation for ΔC_s can be obtained, with soil specific carbon-concentration (β_s) and carbon-climate (γ_s) feedback parameters, which represent the sensitivity of ΔC_s to CO_2 and T, respectively (Equation 7).

2.3 Calculation of feedback parameters

2.3.1 Defining climate variables

For each of the CMIP6 ESMs, the CMIP output variables: *cSoil*, *cLitter*, and *cVeg* are considered in the land carbon storage analysis. Soil carbon (C_s) is defined as the sum of carbon stored in soils and the carbon stored in the litter (CMIP variable *cSoil* + CMIP variable *cLitter*), allowing for a more consistent comparison between the models despite differences in how soil carbon and litter carbon are simulated (Varney et al., 2022; Todd-Brown et al., 2013). For models that do not report a separate litter carbon pool (CMIP variable *cLitter*), soil carbon is taken to be simply the CMIP variable *cSoil* (UKESM1-0-LL). Land carbon (C_L) is defined as the sum of carbon stored in soil + litter (C_s), plus the carbon stored in vegetation (C_v, CMIP variable *cVeg*). Global total values for C_s and C_L (PgC) are calculated using an area weighted sum (using the model land surface fraction, CMIP variable *sftlf*).

Increases in global temperatures (ΔT) are considered using CMIP variable *tas*, which is defined as the change in near-surface air temperature (°C). To calculate changes in atmospheric CO_2 (ΔCO_2) in the C4MIP 1% CO_2 simulations, initial pre-industrial CO_2 concentrations are assumed to be 285 ppm, and then cumulatively increased by 1% each year, for 70 years (approximately 2xCO_2) or 140 years (approximately 4xCO_2).

2.3.2 Carbon-concentration feedback parameter (β)

To calculate the soil carbon-concentration feedback parameter (β_s), the BGC run was used. For each ESM, the change in soil carbon in the BGC run (ΔC_s^{BGC}, PgC) was divided by the change in CO_2 concentration (ppm) up to that point in time

https://doi.org/10.5194/egusphere-2023-2666
Preprint. Discussion started: 15 November 2023

(expressed in units of carbon uptake or release per unit change in CO_2, PgC ppm^{-1}). For this study, β_s was calculated at the time of 2xCO_2 and 4xCO_2. To calculate the land carbon-concentration feedback parameter (β_L), the same method was used but replacing C_s^{BGC} with C_L^{BGC}.

2.3.3 Carbon-climate feedback parameter (γ)

To calculate the soil carbon-climate feedback parameter (γ_s), the RAD run was used. For each ESM, the change in soil carbon in the RAD run (ΔC_s^{RAD}, PgC) was divided by the change in temperature T (°C) up to that point in time (expressed in units of carbon uptake or release per unit change in temperature, PgC °C^{-1}). For this study, γ_s was calculated at 2xCO_2 and 4xCO_2. To calculate the land carbon-climate feedback parameter (γ_L), the same method was used but replacing C_s^{RAD} with C_L^{RAD}.

3 Results

3.1 Projections of soil carbon change

Projections of ΔC_s in CMIP6 ESMs for the full 1% CO_2, biogeochemically coupled (BGC) and radiatively coupled (RAD) simulations are presented in Fig. 1. Soil carbon is projected to increase in the full 1% CO_2 simulation amongst CMIP6 ESMs (ensemble mean 88.2 $\pm$ 40.4 PgC at 2xCO_2 and 177 $\pm$ 141 PgC at 4xCO_2). However, the magnitude of the increase varies amongst the ESMs, with a range of 38 PgC (NorESM2-LM) to 145 PgC (BCC-CSM2-MR) at 2xCO_2, and a range of 15 PgC (ACCESS-ESM1-5) to 502 PgC (CanESM5) at 4xCO_2. Six of the ESMs (CanESM5, CESM2, IPSL-CM6A-LR, MIROC-ES2L, MPI-ESM1-2-LR, NorESM2-LM) see an increased ΔC_s value with increasing climate forcing, however the remaining four ESMs (ACCESS-ESM1-5, BCC-CSM2-MR, GFDL-ESM4, UKESM1-0-LL) see a saturation to the rate of increase, or even a turning point where carbon starts to decrease again, from 70 years ($\approx$ 2xCO_2) in the simulation (Fig. 1(a)).

The projected increase in ΔC_s is the net effect of the increases projected in the BGC run (ensemble mean 132 $\pm$ 66.5 PgC at 2xCO_2 and 348 $\pm$ 203 PgC at 4xCO_2, Fig. 1(b)) and the decreases projected in the RAD run (ensemble mean -45.5 $\pm$ 22.9 PgC at 2xCO_2 and -170 $\pm$ 94.7 PgC at 4xCO_2, Fig. 1(c)). The response due to increases in atmospheric CO_2 (BGC simulation) are found to dominate the overall response (full 1% CO_2 simulation) in the majority of models, where greater magnitudes of change are seen compared to the RAD simulation (exception ACCESS-ESM1-5). The BGC simulation also sees a greater spread in projected ΔC_s, with a range of 218 PgC at 2xCO_2 and 603 PgC at 4xCO_2, compared to ranges of 68 PgC at 2xCO_2 and 312 PgC at 4xCO_2 in the RAD simulation.

Fig. 2 shows patterns of ΔC_s changes at 4xCO_2 for the full 1% CO_2, BGC and RAD simulations. In the BGC simulation, increases in ΔC_s are seen across the majority of regions within CMIP6 ESMs, though exceptions are found in the northern latitudes for two ESMs (CanESM5 and NorESM2-LM). Across the ensemble, the projected increases in ΔC_s have spatially varying magnitudes, where generally the greatest increases are seen in the tropical regions. Conversely, the RAD simulation generally sees reductions in ΔC_s globally, with the greatest reductions seen in the tropical regions. However, disagreement is seen in the northern latitudes, where four models (ACCESS-ESM1-5, CanESM5, MIROC-ES2L, UKESM1-0-LL) see an

https://doi.org/10.5194/egusphere-2023-2666
Preprint. Discussion started: 15 November 2023

increased ΔC_s and three models (BCC-CSM2-MR, CESM2, NorESM2-LM) see a decreased ΔC_s. The overall ΔC_s values seen in the full 1% CO_2 simulation are again found to be mostly dominated by the BGC simulation (Fig. 2), though exceptions are seen where the RAD simulation is shown to dominate the response for certain regions. Specifically, the reduced ΔC_s within the RAD simulation dominates the net response in the northern latitudes of three ESMs (BCC-CSM2-MR, CESM2, and NorESM2-LM; the only models where decreases where seen), as well as in the tropical regions of a different three ESMs (ACCESS-ESM1-5, GFDL-ESM4, and UKESM1-0-LL).

3.2 Soil carbon-concentration and carbon-climate feedback parameters

The sensitivity of soil carbon to changes in atmospheric CO_2 (BGC simulation) and global temperatures (RAD simulation) can be quantified using soil carbon specific carbon-concentration (β_s) and carbon-climate (γ_s) feedback parameters, respectively. These were calculated for each CMIP6 ESM and the values are presented in Table 2. Values for β_s are found to be positive amongst the CMIP6 ESMs which is consistent with increased C_s with increasing CO_2, and values for γ_s are found to be negative which is consistent with decreased C_s with increasing temperature (Fig. 3).

The magnitude of the feedback parameters (β_s and γ_s) are found to vary amongst the CMIP6 ensemble, suggesting uncertainty in the magnitude of the soil carbon response to climate change. Generally, models with higher sensitivities to CO_2 (β_s), also have higher sensitivities to temperature (γ_s), where a r^2 values of 0.64 ($2xCO_2$) and 0.60 ($4xCO_2$) are found between the β_s and γ_s values (Table 2). The range in projected β_s parameters are found to be relatively consistent between $2xCO_2$ and $4xCO_2$ (where a small decrease is seen), with a range of 0.704 PgC ppm^{-1} and range of 0.636 PgC ppm^{-1} respectively. Conversely, the range of calculated γ_s parameters are found to be less consistent between $2xCO_2$ and $4xCO_2$ (increasing range with increased CO_2), with ranges of 42.7 PgC $°C^{-1}$ and 68.0 PgC $°C^{-1}$ respectively (Table 2).

The linearity of future soil carbon changes can be investigated by comparing the $2xCO_2$ and $4xCO_2$ lines for β_s and γ_s in Fig. 3. A future linear response is shown to be a good approximation, however the figure suggests a slight non-linearity in the soil carbon response to both CO_2 (ΔC_s^{BGC}) and temperature (ΔC_s^{RAD}) in the majority of ESMs. The BGC simulation generally sees greater consistency between $2xCO_2$ and $4xCO_2$ β_s values, for example in the CESM2 and NorESM2-LM models. However, the majority of ESMs (ACCESS-ESM1-5, BCC-CSM2-MR, GFDL-ESM4, IPSL-CM6A-LR, MIROC-ES2L, MPI-ESM1-2-LR, and UKESM1-0-LL) see a reduction in β_s and a saturation to the sensitivity with greater CO_2 levels (Fig. 3(a)). In the RAD simulation, generally inconsistencies are seen between $2xCO_2$ and $4xCO_2$ (exception MPI-ESM1-2-LR) and an increased sensitivity of C_s^{RAD} to temperature (T) with increased climate forcing is suggested by the majority of CMIP6 ESMs (Fig. 3(b)). As an example, in CESM2 where one of the lowest sensitivities to T at $2xCO_2$ is seen, the ESM see an approximate 50% increase in γ_s by $4xCO_2$ (Table 2).

3.3 Investigating robustness of the ΔC_s approximation

The projected change in soil carbon (ΔC_s) in ESMs in the full 1% CO_2 simulation was compared with the estimated ΔC_s derived using Equation 7, which uses the derived β_s and γ_s feedback parameters together with model specific ΔT and estimates for ΔCO_2 (Fig. 4). This investigates the approximation that changes in the full 1% CO_2 simulation is equal to the sum of

https://doi.org/10.5194/egusphere-2023-2666
Preprint. Discussion started: 15 November 2023

changes in the BGC and RAD simulations. At 2xCO$_2$, the approximation is found to predict ΔC_s within 20% of the actual projected values in the 1% CO$_2$ simulation for 7 out of the 10 CMIP6 ESMs (BCC-CSM2-MR, CESM2, GFDL-ESM4, IPSL-CM6A-LR, MIROC-ES2L, MPI-ESM1-2-LR and UKESM1-0-LL). At 4xCO$_2$, the robustness of the assumption between the BGC and RAD simulations reduces for future changes in soil carbon. However, $\beta_s \Delta CO_2 + \gamma_s \Delta T$ is within 20% of the projected ΔC_s for 5 out of the 10 ESMs (GFDL-ESM4, IPSL-CM6A-LR, MIROC-ES2L, MPI-ESM1-2-LR and UKESM1-0-LL). The models where the approximation is the least consistent with projected ΔC_s are ACCESS-ESM1-5 and BCC-CSM2-MR, where at 4xCO$_2$ the greatest non-linearities are present between BGC and RAD simulations.

3.4 Comparisons between soil and land feedback parameters

The contribution of the sensitivity of soil carbon stocks (C_s) to the total sensitivity of land carbon stocks (C_L) was investigated by comparing the β and γ feedback parameters for land (Table A1) and soil (Table 2), for both 2xCO$_2$ and 4xCO$_2$ (Fig. 5). Here, the assumption from Equation 5 is followed that the land sensitivity is made up of the sum of the soil and vegetation responses. For the carbon-concentration feedback (β), the portion of the land sensitivity to CO$_2$ (β_L) that is due to global soils (β_s) ranges from 19% (NorESM2-LM) to 53% (BCC-CSM2-MR), with a mean of 38 $\pm$ 11 % seen across the CMIP6 ESMs at 2xCO$_2$ (Fig. 5(a)). Similar proportions are found at 4xCO$_2$, ranging from 22% (NorESM2-LM) to 58% (MIROC-ES2-L), with a mean of 42 $\pm$ 12 % seen across the CMIP6 ESMs (Fig. 5(b)). The portion of β_L due to β_s is estimated to be close to half the total land response. For the carbon-climate feedback (γ), the portion of the land sensitivity to climate (γ_L) that is due to global soils (γ_s) ranges from approximately 42% (CESM2) to 147% (MPI-ESM1-2-LM), with a mean of 75 $\pm$ 30 % seen across the CMIP6 ESMs at 2xCO$_2$ (Fig. 5(a)), and at 4xCO$_2$ the ranges is from 48% (ACCESS-ESM1-5) to 157% (MPI-ESM1-2-LM), with a mean of 75 $\pm$ 31 % seen across the CMIP6 ESMs (Fig. 5(b)). Therefore, the portion of γ_L due to γ_s is estimated to be the majority of the sensitivity, suggesting that soil dominates the response of land carbon to climate. Note that the MPI-ESM1-2-LR model sees a greater γ_s value compared with γ_L, resulting in the percentage of the land response attributed to soil being greater than 100%. This suggests a positive γ_v response in this model, meaning a predicted increased vegetation carbon with global warming.

4 Discussion

Quantifying the future sensitivity of global soil carbon stocks to anthropogenic CO$_2$ emissions and their role within future land carbon storage is vital in order to understand future changes in the Earth's climate system (Canadell et al., 2021). Global changes in soil carbon (ΔC_s), in the absence of human disturbance and land-use change, will result from responses due to changes in atmospheric CO$_2$ and associated changes in global temperatures (T), which is used to represent climate effects on a global scale. By separating the sensitivities due to increasing CO$_2$ and T, the idealised C4MIP ESM simulations allows for these effects on soil carbon to be examined individually and the use of the $\beta\gamma$ formulation allows these sensitivities to be quantified and compared for CMIP6 ESMs (See Methods; Jones et al. (2016); Friedlingstein et al. (2006)).

https://doi.org/10.5194/egusphere-2023-2666
Preprint. Discussion started: 15 November 2023

Across CMIP6 ESMs, soil carbon is projected to increase in the BGC simulation ('CO_2 only') and decrease in the RAD simulation ('climate only'), consistent with projections of the overall land carbon response (Arora et al., 2020). The BGC simulation has been used to quantify the sensitivity of soil carbon to ΔCO_2 (β_s), where positive β_s values were defined due to the projected increase in soil carbon with increased atmospheric CO_2 (Fig. 1(b)). This is known to be due to an increased CO_2 fertilisation effect on land, which is the term used to explain an increased productivity of vegetation under higher atmospheric CO_2 concentrations. This is known to lead to an increased input of litter carbon into soil carbon pools (Schimel et al., 2015; Koven et al., 2015), though how well models represent the allocation of the land carbon uptake between plants and soils is debated (Terrer et al., 2021). It has been shown that an increased rate of carbon input into the soil within ESMs also results in a transient reduction in soil carbon; a phenomenon known as false priming (Koven et al., 2015), however the magnitude of this effect has been shown to be small compared to the resultant CO_2 fertilisation effect within CMIP6 (Varney et al., 2023). Despite agreement on a net increase in soil carbon stocks (positive β_s) globally, this study highlights uncertainty on the projected magnitude of this sensitivity amongst the CMIP6 models (Table 2).

The RAD simulation has been used to quantify the sensitivity of soil carbon to changes in climate (ΔT; γ_s), where negative γ_s values were defined due to the projected decrease in soil carbon with global warming (Fig. 1(c)). On a global scale, the reduction in soil carbon under climate changes is known to be due to an increased rate of heterotrophic respiration (R_h) under warmer temperatures (Crowther et al., 2016; Todd-Brown et al., 2014). Spatially however, climate induced ΔC_s is known to vary and can result in both increases and decreases in soil carbon (Fig. 2). For example, increased temperatures in northern latitudes could result in the northward expansion of boreal forests (Pugh et al., 2018), which would increase forest productivity and subsequently carbon storage in these regions. Conversely, future changes in precipitation patterns could lead to regions with reduced soil moisture, which would lead to reduced vegetation productivity and carbon uptake (Green et al., 2019). The uncertainties in projected spatial changes, as well uncertainties in carbon turnover times within the soil (Arora et al., 2020; Varney et al., 2020; Koven et al., 2017), leads to differences in the projected magnitude of the γ_s sensitivity amongst the CMIP6 models (Table 2).

This paper highlights the importance of soils within the role of the land surface response to global warming (Fig. 5). Despite the CO_2 sensitivity of ΔC_s dominating net soil carbon changes (β_s), it could be argued that the significance of the soil climate sensitivity will increase under more extreme levels of climate change (γ_s). This is suggested by both a projected saturation of β_s and an increase in γ_s, between 2xCO_2 and 4xCO_2 shown in the CMIP6 ensemble means (Table 2). The saturation, or reduced rate of increase, in β_s seen in CMIP6 is likely due to a limit of the CO_2 fertilisation effect. The rate of CO_2 fertilisation in the future is expected to be limited by nutrient availability (Wieder et al., 2015), which in CMIP6 is now more explicitly represented by the inclusion of an interactive nitrogen cycle in multiple models (Table 1). This implementation is expected to limit the increased productivity from CO_2 fertilisation within ESMs (Davies-Barnard et al., 2020), and has previously been found to lower the magnitude of the land feedback parameters (Arora et al., 2020).

Conversely, the sensitivity of soil carbon to climate changes has been shown to increase with global warming, where the greater γ_s at 4xCO_2 compared to 2xCO_2 implies a greater rate of soil carbon loss under increased global temperature. Furthermore, limitations within CMIP6 ESMs in the representation of soil carbon and related processes could suggest a potential

https://doi.org/10.5194/egusphere-2023-2666
Preprint. Discussion started: 15 November 2023

underestimation of γ_s. In Fig. 2, reductions in soil carbon stocks are shown in the full 1% simulation within the high northern latitudes for only 3 models considered in this study (BCC-CSM2-MR, CESM2, and NorESM2-LM). These models have previously been shown to be the only CMIP6 models to represent quantities of northern latitude carbon stocks consistently with observational estimates (Varney et al., 2022), which suggests an increased likelihood of soil carbon loss from the northern latitudes when historical stocks are represented more consistently with observations. It is noted that CESM2 and NorESM2-LM contain the same land surface component so are expected to show similar results (Lawrence et al., 2019). Moreover, the majority of ESMs do not include implicit representation of permafrost carbon (Burke et al., 2020), which means large quantities of carbon which are known to be especially sensitive to global warming, are not included in the calculation of these feedbacks (Schuur et al., 2015).

The $\beta\gamma$ formulation has many benefits in allowing the quantification and comparison of land and soil carbon feedbacks amongst ESMs. However, non-linearities between the CO_2 and T responses are known and have previously been shown within ESMs in the future land carbon responses (Schwinger et al., 2014; Zickfeld et al., 2011; Gregory et al., 2009). Zickfeld et al. (2011) suggest that the non-linearity in the land response are due to significantly differing vegetation responses which depend on whether or not climate effects are combined with the CO_2 fertilisation effect; for example, forest dieback (Cox et al., 2004). However, this is model dependent as not all models within CMIP6 simulate dynamic vegetation (Table 1). The spatial variations in the response of soil carbon to CO_2 and climate that are seen in Fig. 2 could also contribute to the non-linearity. For example, a different spatial pattern of soil carbon under elevated CO_2 could lead to a different overall temperature response, e.g. if more carbon is in the high latitudes where greater temperature changes are seen. Arora et al. (2020) find that climate responses in the BGC simulation account for a difference of 1% - 5% in the calculation of the feedbacks, suggesting a small but non-negligible effect of climate in the BGC runs. This response was shown to be dependent on the representation of vegetation within the model, as with the non-linearities found in Zickfeld et al. (2011). Despite this, isolating and quantifying the key sensitivities with the $\beta\gamma$ method provides a useful benchmark for feedbacks within CMIP.

5 Conclusions

The Friedlingstein et al. (2006) methodology adapted in this study suggests that β_s and γ_s is a valid assumption for projected soil carbon changes in ESMs up until a doubling of CO_2. However, under more extreme levels of climate change, the results here suggest the need for the non-linearity in feedbacks to be further investigated. Soil carbon is found to have a greater impact on carbon-climate feedbacks than vegetation carbon responses, which means that the sensitivity of soil to changes in global temperature is the dominant response of the land surface. Therefore, further understanding and quantifying the sensitivity of global soils under global warming is necessary to quantify future changes in the climate system. Moreover, the sensitivity of soil carbon to temperature increases with increasing climate forcing, suggesting that soil carbon is particularly important in the long-term response of land carbon storage under extreme levels of global warming.

https://doi.org/10.5194/egusphere-2023-2666
Preprint. Discussion started: 15 November 2023

Code availability. Code is available on GitHub (https://github.com/rebeccamayvarney/CMIP6-soil-beta-gamma).

Data availability. The CMIP6 data analysed during this study is available online (https: //esgf-node.llnl.gov/search/cmip6/).

Author contributions. RMV and PMC outlined the study. RMV completed the analysis and produced the figures. All the co-authors provided guidance on the study at various times and suggested edits to the draft manuscript.

Competing interests. The authors have declared no competing interests.

Acknowledgements. This research has been supported by the European Research Council, Climate–Carbon Interactions in the Current Century project (4C; grant no. 821003) (RMV, PMC and PF) and Emergent Constraints on Climate–Land feedbacks in the Earth System project (ECCLES; grant no. 742472) (RMV and PMC). SEC was supported by a Natural Environment Research Council independent research fellowship (grant no. NE/R015791/1). EJB was supported by the Joint UK BEIS/Defra Met Office Hadley Centre Climate Programme (grant no. GA01101). We thank the World Climate Research Programme's Working Group on Coupled Modelling and the climate modelling groups for producing and making their model output available.

https://doi.org/10.5194/egusphere-2023-2666
Preprint. Discussion started: 15 November 2023

References

Arora, V. K., Boer, G. J., Friedlingstein, P., Eby, M., Jones, C. D., Christian, J. R., Bonan, G., Bopp, L., Brovkin, V., Cadule, P., et al.: Carbon–concentration and carbon–climate feedbacks in CMIP5 Earth system models, Journal of Climate, 26, 5289–5314, 2013.

Arora, V. K., Katavouta, A., Williams, R. G., Jones, C. D., Brovkin, V., Friedlingstein, P., Schwinger, J., Bopp, L., Boucher, O., Cadule, P., et al.: Carbon–concentration and carbon–climate feedbacks in CMIP6 models and their comparison to CMIP5 models, Biogeosciences, 17, 4173–4222, 2020.

Boer, G. and Arora, V.: Feedbacks in emission-driven and concentration-driven global carbon budgets, Journal of climate, 26, 3326–3341, 2013.

Burke, E. J., Zhang, Y., and Krinner, G.: Evaluating permafrost physics in the Coupled Model Intercomparison Project 6 (CMIP6) models and their sensitivity to climate change, The Cryosphere, 14, 3155–3174, 2020.

Canadell, J., Monteiro, P., Costa, M., Cotrim da Cunha, L., Cox, P., Eliseev, A., Henson, S., Ishii, M., Jaccard, S., Koven, C., Lohila, A., Patra, P., Piao, S., Rogelj, J., Syampungani, S., Zaehle, S., and Zickfeld, K.: Global Carbon and other Biogeochemical Cycles and Feedbacks, Cambridge University Press, Cambridge, United Kingdom and New York, NY, USA, https://doi.org/10.1017/9781009157896.007, 2021.

Cox, P. M., Betts, R., Collins, M., Harris, P. P., Huntingford, C., and Jones, C.: Amazonian forest dieback under climate-carbon cycle projections for the 21st century, Theoretical and applied climatology, 78, 137–156, 2004.

Crowther, T. W., Todd-Brown, K. E., Rowe, C. W., Wieder, W. R., Carey, J. C., Machmuller, M. B., Snoek, B., Fang, S., Zhou, G., Allison, S. D., et al.: Quantifying global soil carbon losses in response to warming, Nature, 540, 104–108, 2016.

Davies-Barnard, T., Meyerholt, J., Zaehle, S., Friedlingstein, P., Brovkin, V., Fan, Y., Fisher, R. A., Jones, C. D., Lee, H., Peano, D., et al.: Nitrogen cycling in CMIP6 land surface models: progress and limitations, Biogeosciences, 17, 5129–5148, 2020.

Eyring, V., Bony, S., Meehl, G. A., Senior, C. A., Stevens, B., Stouffer, R. J., and Taylor, K. E.: Overview of the Coupled Model Intercomparison Project Phase 6 (CMIP6) experimental design and organization, Geoscientific Model Development (Online), 9, 2016.

Friedlingstein, P., Dufresne, J.-L., Cox, P., and Rayner, P.: How positive is the feedback between climate change and the carbon cycle?, Tellus B: Chemical and Physical Meteorology, 55, 692–700, 2003.

Friedlingstein, P., Cox, P., Betts, R., Bopp, L., von Bloh, W., Brovkin, V., Cadule, P., Doney, S., Eby, M., Fung, I., et al.: Climate–carbon cycle feedback analysis: results from the C4MIP model intercomparison, Journal of climate, 19, 3337–3353, 2006.

Friedlingstein, P., O'sullivan, M., Jones, M. W., Andrew, R. M., Gregor, L., Hauck, J., Le Quéré, C., Luijkx, I. T., Olsen, A., Peters, G. P., et al.: Global carbon budget 2022, Earth System Science Data, 14, 4811–4900, 2022.

Green, J. K., Seneviratne, S. I., Berg, A. M., Findell, K. L., Hagemann, S., Lawrence, D. M., and Gentine, P.: Large influence of soil moisture on long-term terrestrial carbon uptake, Nature, 565, 476–479, 2019.

Gregory, J. M., Jones, C., Cadule, P., and Friedlingstein, P.: Quantifying carbon cycle feedbacks, Journal of Climate, 22, 5232–5250, 2009.

IPCC: Climate Change 2021: The Physical Science Basis. Contribution of Working Group I to the Sixth Assessment Report of the Intergovernmental Panel on Climate Change, Cambridge University Press, Cambridge, UK and New York, NY, USA, https://doi.org/10.1017/9781009157896, 2021.

Jones, C. D., Arora, V., Friedlingstein, P., Bopp, L., Brovkin, V., Dunne, J., Graven, H., Hoffman, F., Ilyina, T., John, J. G., et al.: C4MIP–The coupled climate–carbon cycle model intercomparison project: Experimental protocol for CMIP6, Geoscientific Model Development, 9, 2853–2880, 2016.

https://doi.org/10.5194/egusphere-2023-2666
Preprint. Discussion started: 15 November 2023

Koven, C. D., Chambers, J. Q., Georgiou, K., Knox, R., Negron-Juarez, R., Riley, W. J., Arora, V. K., Brovkin, V., Friedlingstein, P., and Jones, C. D.: Controls on terrestrial carbon feedbacks by productivity versus turnover in the CMIP5 Earth System Models, Biogeosciences, 12, 5211–5228, https://doi.org/10.5194/bg-12-5211-2015, 2015.

Koven, C. D., Hugelius, G., Lawrence, D. M., and Wieder, W. R.: Higher climatological temperature sensitivity of soil carbon in cold than warm climates, Nature Climate Change, 7, 817–822, 2017.

Lawrence, D. M., Fisher, R. A., Koven, C. D., Oleson, K. W., Swenson, S. C., Bonan, G., Collier, N., Ghimire, B., van Kampenhout, L., Kennedy, D., et al.: The Community Land Model version 5: Description of new features, benchmarking, and impact of forcing uncertainty, Journal of Advances in Modeling Earth Systems, 11, 4245–4287, 2019.

Pugh, T., Jones, C., Huntingford, C., Burton, C., Arneth, A., Brovkin, V., Ciais, P., Lomas, M., Robertson, E., Piao, S., et al.: A large committed long-term sink of carbon due to vegetation dynamics, Earth's Future, 6, 1413–1432, 2018.

Schimel, D., Pavlick, R., Fisher, J. B., Asner, G. P., Saatchi, S., Townsend, P., Miller, C., Frankenberg, C., Hibbard, K., and Cox, P.: Observing terrestrial ecosystems and the carbon cycle from space, Global Change Biology, 21, 1762–1776, 2015.

Schuur, E. A., McGuire, A. D., Schädel, C., Grosse, G., Harden, J. W., Hayes, D. J., Hugelius, G., Koven, C. D., Kuhry, P., Lawrence, D. M., et al.: Climate change and the permafrost carbon feedback, Nature, 520, 171–179, 2015.

Schwinger, J., Tjiputra, J. F., Heinze, C., Bopp, L., Christian, J. R., Gehlen, M., Ilyina, T., Jones, C. D., Salas-Mélia, D., Segschneider, J., et al.: Nonlinearity of ocean carbon cycle feedbacks in CMIP5 earth system models, Journal of Climate, 27, 3869–3888, 2014.

Terrer, C., Phillips, R. P., Hungate, B. A., Rosende, J., Pett-Ridge, J., Craig, M. E., van Groenigen, K. J., Keenan, T. F., Sulman, B. N., Stocker, B. D., et al.: A trade-off between plant and soil carbon storage under elevated CO2, Nature, 591, 599–603, 2021.

Todd-Brown, K., Randerson, J., Post, W., Hoffman, F., Tarnocai, C., Schuur, E., and Allison, S.: Causes of variation in soil carbon simulations from CMIP5 Earth system models and comparison with observations, Biogeosciences, 10, 1717–1736, 2013.

Todd-Brown, K., Randerson, J., Hopkins, F., Arora, V., Hajima, T., Jones, C., Shevliakova, E., Tjiputra, J., Volodin, E., Wu, T., et al.: Changes in soil organic carbon storage predicted by Earth system models during the 21st century, Biogeosciences, 11, 2341–2356, 2014.

Varney, R. M., Chadburn, S. E., Friedlingstein, P., Burke, E. J., Koven, C. D., Hugelius, G., and Cox, P. M.: A spatial emergent constraint on the sensitivity of soil carbon turnover to global warming, Nature communications, 11, 5544, 2020.

Varney, R. M., Chadburn, S. E., Burke, E. J., and Cox, P. M.: Evaluation of soil carbon simulation in CMIP6 Earth system models, Biogeosciences, 19, 4671–4704, https://doi.org/10.5194/bg-19-4671-2022, 2022.

Varney, R. M., Chadburn, S. E., Burke, E. J., Jones, S., Wiltshire, A. J., and Cox, P. M.: Simulated responses of soil carbon to climate change in CMIP6 Earth System Models: the role of false priming, Biogeosciences, 20, 3767–3790, 2023.

Wieder, W. R., Cleveland, C. C., Lawrence, D. M., and Bonan, G. B.: Effects of model structural uncertainty on carbon cycle projections: biological nitrogen fixation as a case study, Environmental Research Letters, 10, 044 016, 2015.

Zickfeld, K., Eby, M., Matthews, H. D., Schmittner, A., and Weaver, A. J.: Nonlinearity of carbon cycle feedbacks, Journal of Climate, 24, 4255–4275, 2011.

https://doi.org/10.5194/egusphere-2023-2666
Preprint. Discussion started: 15 November 2023

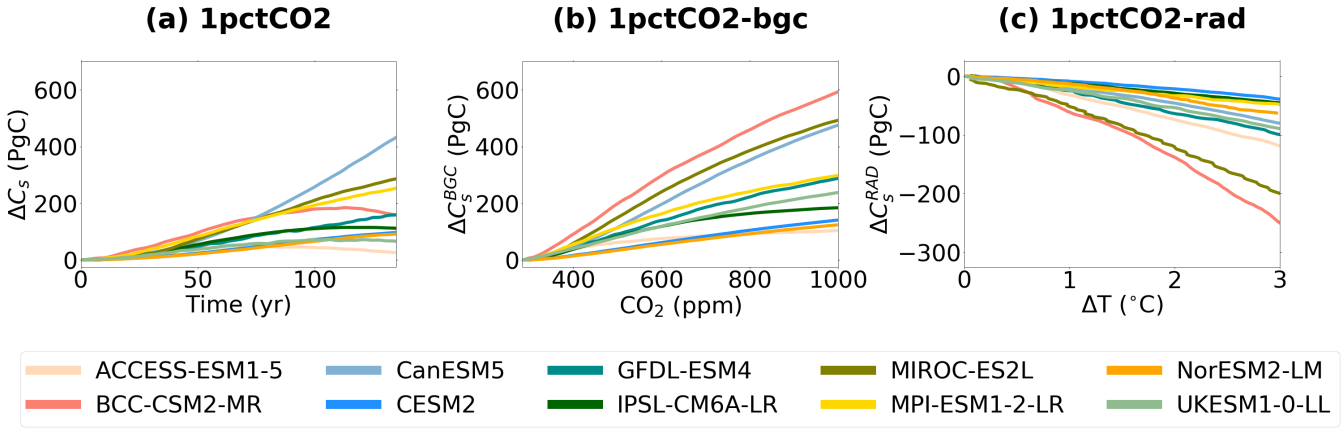

Figure 1. Timeseries of projected changes in soil carbon (ΔC_s) in CMIP6 ESMs, for the: (a) idealised 1% CO_2 (left column), (b) biogeochemically coupled 1% CO_2 (BGC, middle column), and (c) radiatively coupled 1% CO_2 (RAD, right column) simulations.

https://doi.org/10.5194/egusphere-2023-2666
Preprint. Discussion started: 15 November 2023

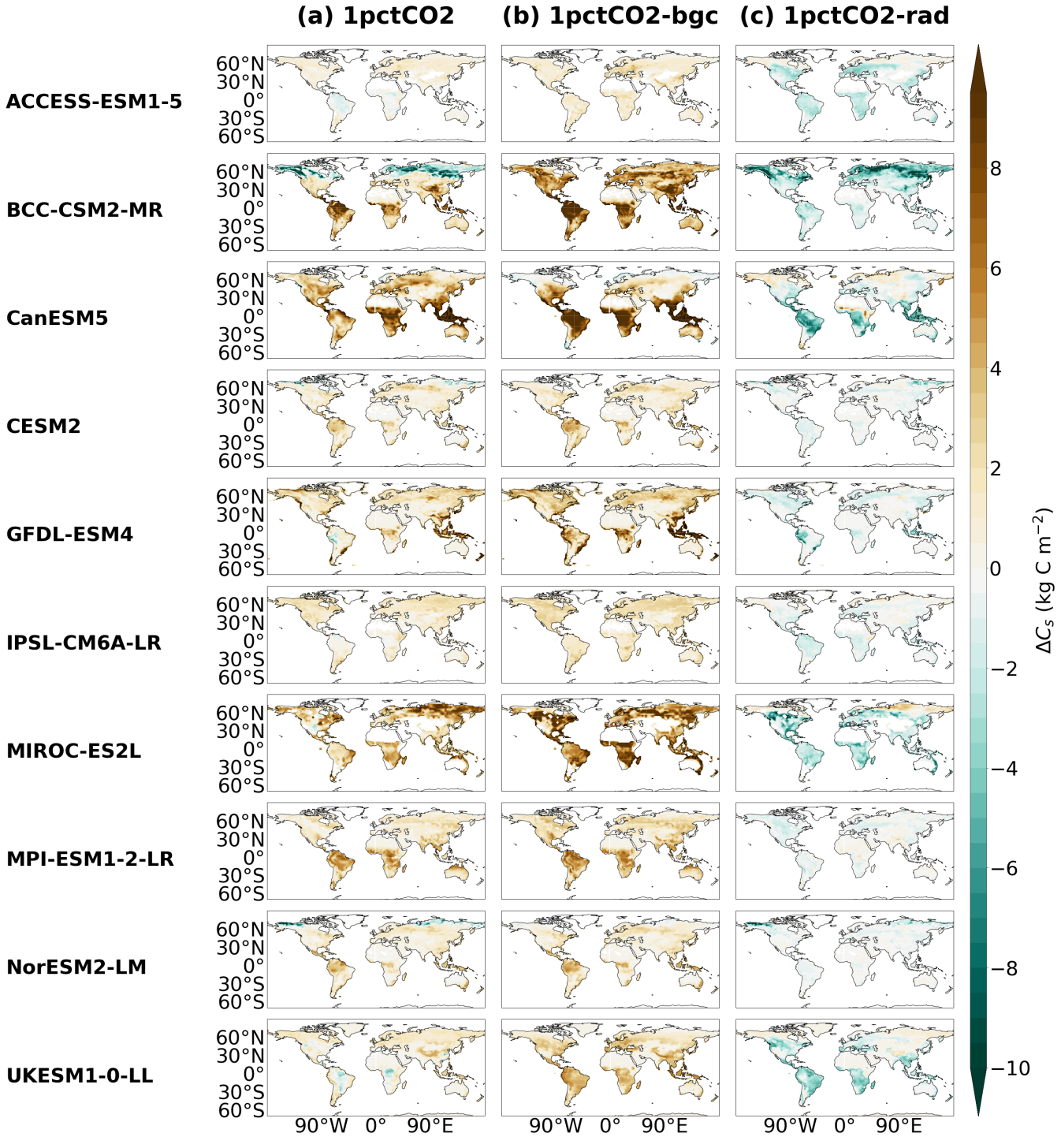

Figure 2. Maps of changes in soil carbon (ΔC_s) at 4xCO_2 in CMIP6 ESMs, for the: (a) idealised simulations 1% CO_2 (left column), (b) biogeochemically coupled 1% CO_2 (BGC, middle column), and (c) radiatively coupled 1% CO_2 (RAD, right column).

https://doi.org/10.5194/egusphere-2023-2666
Preprint. Discussion started: 15 November 2023

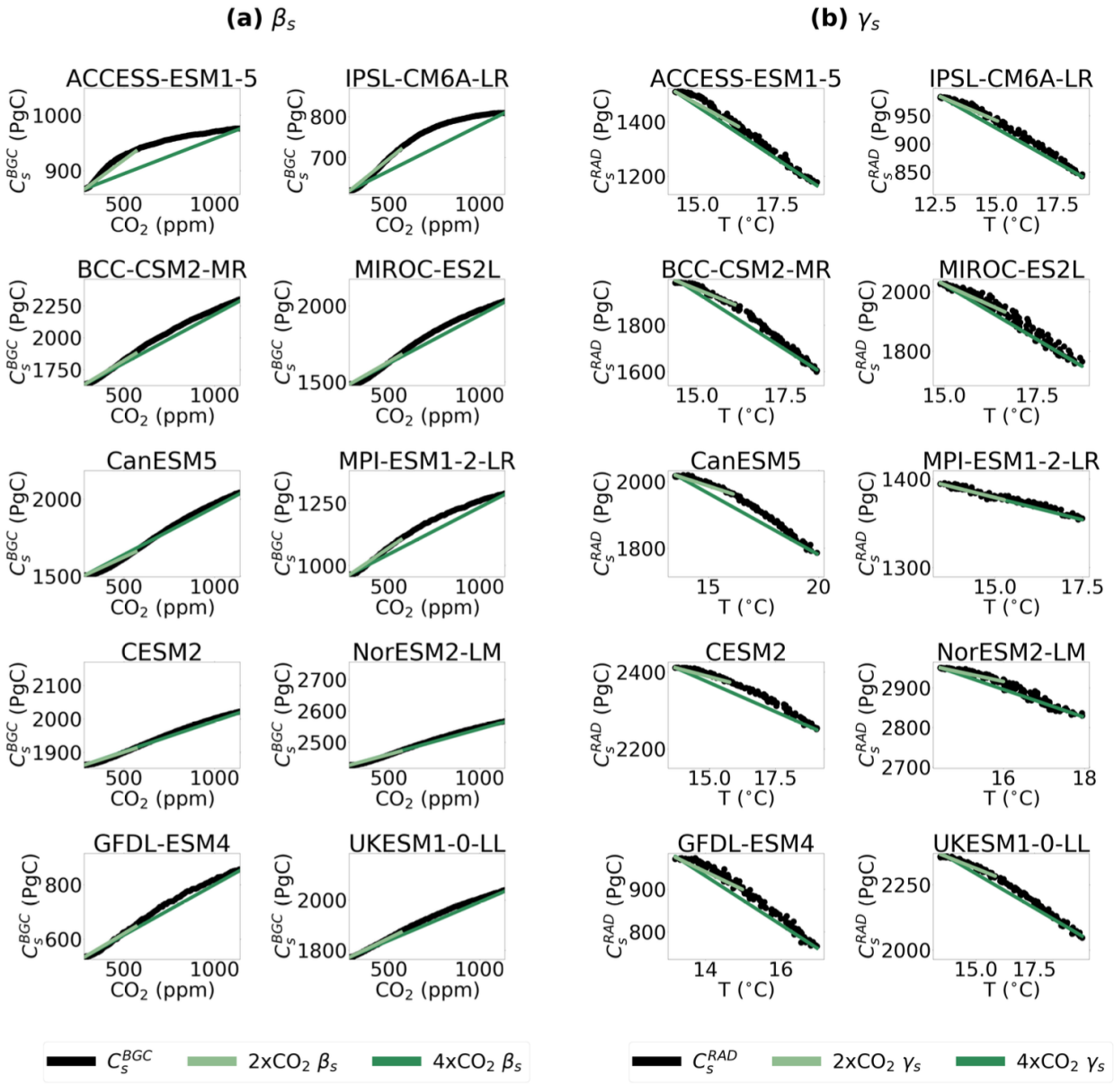

Figure 3. Timeseries plots used to calculate the soil feedback parameters. (a) Soil carbon in the BGC simulation (C_s^{BGC}, PgC) Vs CO_2 (ppm) for the carbon-concentration feedback parameters (β_s, PgC ppm^{-1}), and (b) Soil carbon in the RAD simulation (C_s^{RAD}, PgC) Vs temperature (T, °C) for the soil carbon-climate feedback parameters (γ_s, PgC °C^{-1}), for each CMIP6 ESM.

https://doi.org/10.5194/egusphere-2023-2666
Preprint. Discussion started: 15 November 2023

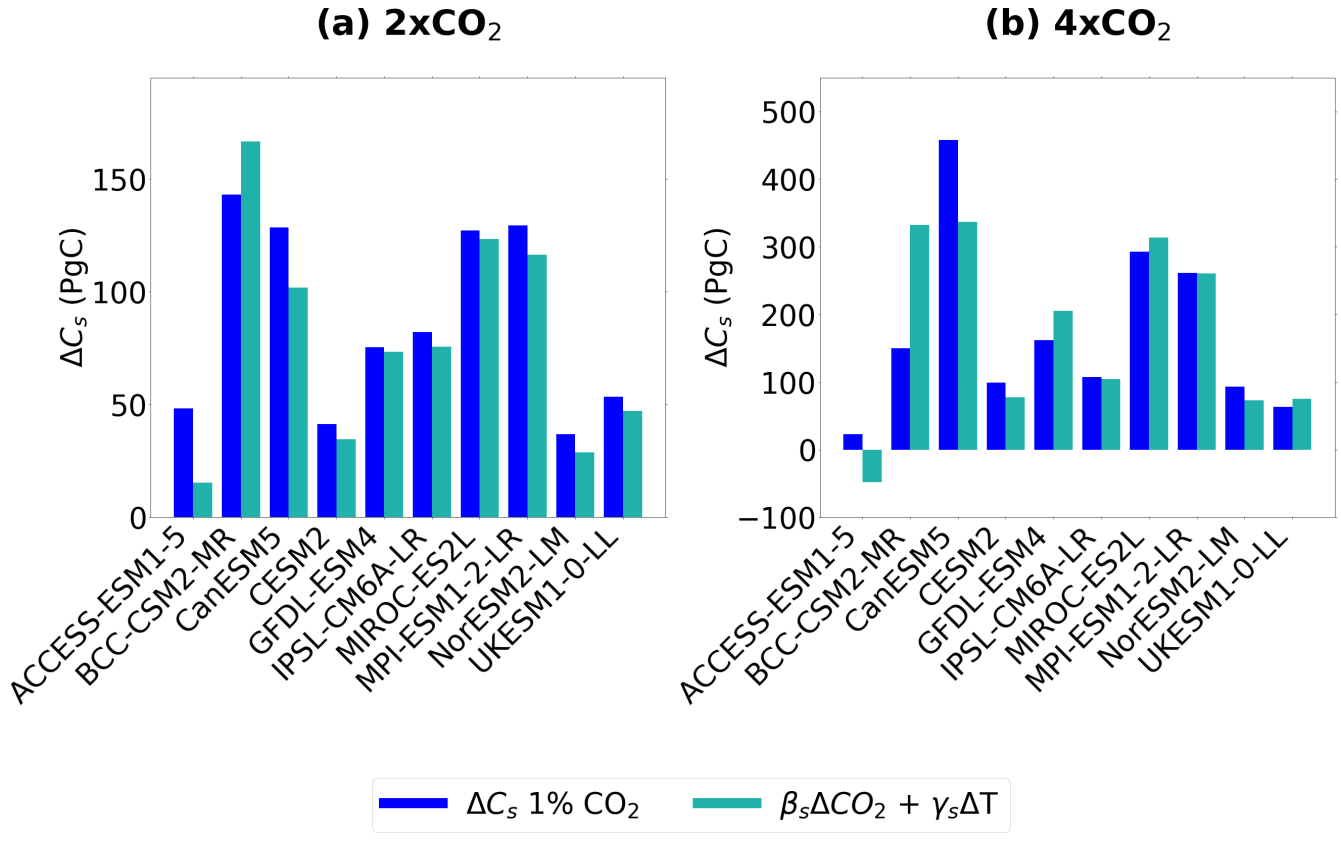

Figure 4. Bar charts comparing ΔC_s (PgC) in the full 1% CO_2 simulations with the estimated ΔC_s using the calculated β_s and γ_s feedback parameters for each CMIP6 ESM, where estimated $\Delta C_s \approx \beta_s \Delta CO_2 + \gamma_s \Delta T$, for (a) 2x$CO_2$ and (b) 4xCO_2.

https://doi.org/10.5194/egusphere-2023-2666
Preprint. Discussion started: 15 November 2023

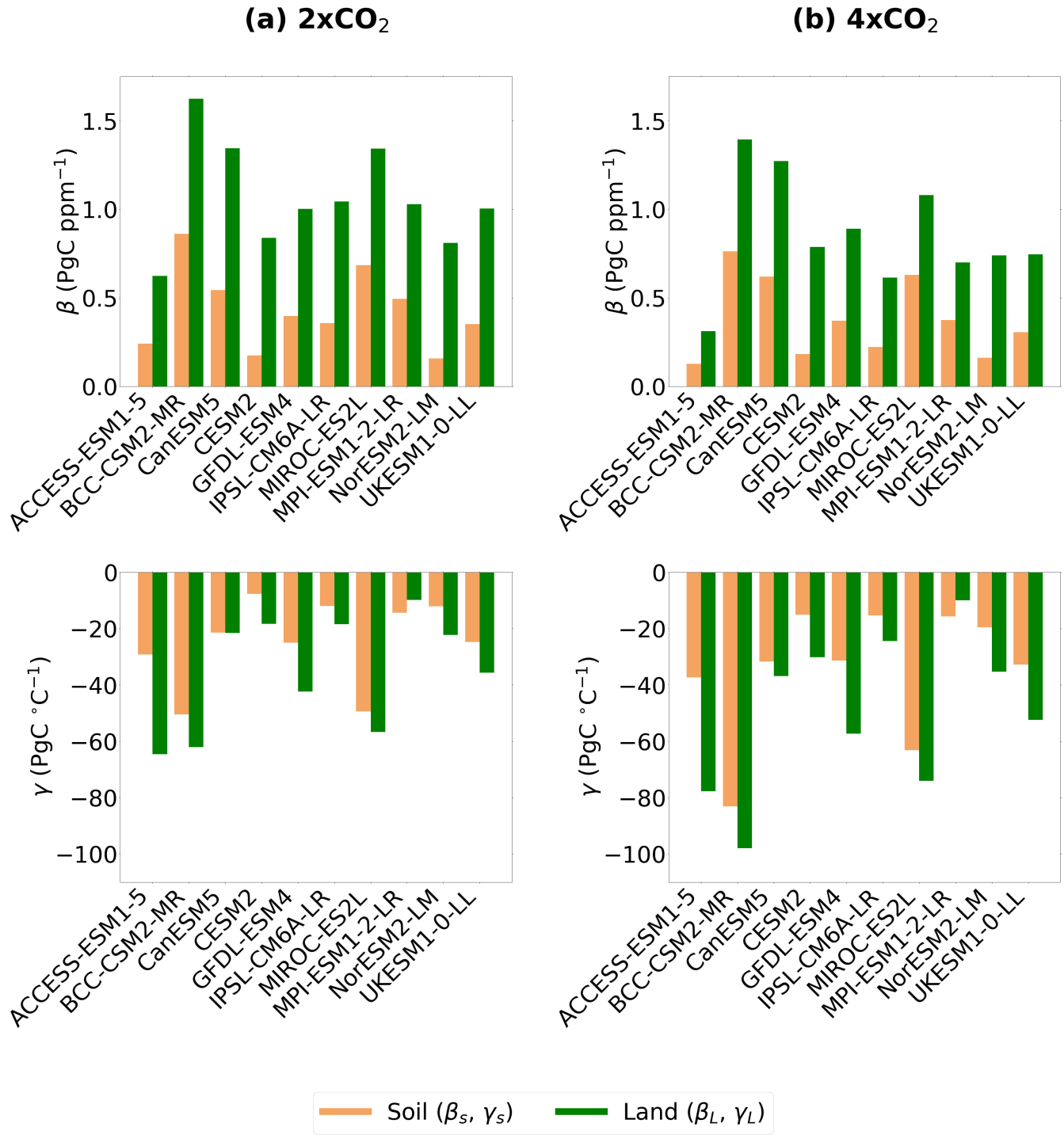

Figure 5. Bar charts comparing the land carbon-concentration (β_L) feedback parameters with the soil carbon-concentration (β_s) feedback parameters (top row), and the land carbon-climate (γ_L) feedback parameters with the soil carbon-climate (γ_s) feedback parameters (bottom row), for (a) 2xCO$_2$ and (b) 4xCO$_2$.

https://doi.org/10.5194/egusphere-2023-2666
Preprint. Discussion started: 15 November 2023

Table 1. The CMIP6 Earth system models included in this study and the relevant features of associated land carbon cycle components: simulation of interactive nitrogen, the inclusion of dynamic vegetation, representation of fire, and the soil decomposition functions used (Varney et al., 2022; Arora et al., 2020). Explanations of the temperature and moisture functions used within ESMs are given in Varney et al. (2022) and Todd-Brown et al. (2013).

Earth System Model	Nitrogen Cycle	Dynamic Vegetation	Fire	Temperature & Moisture Functions
ACCESS-ESM1.5	Yes	No	No	Arrhenius & Hill
BCC-CSM2-MR	No	No	No	Hill & Hill
CanESM5	No	No	No	Q_{10} & Hill
CESM2	Yes	No	Yes	Arrhenius & Increasing
GFDL-ESM4	No	Yes	Yes	Hill & Increasing
IPSL-CM6A-LR	No	No	No	Q_{10} & Increasing
MIROC-ES2L	Yes	No	No	Arrhenius & Increasing
MPI-ESM1.2-LR	Yes	Yes	Yes	Q_{10} & Increasing
NorESM2-LM	Yes	No	Yes	Arrhenius & Increasing
UKESM1-0-LL	Yes	Yes	No	Q_{10} & Hill

https://doi.org/10.5194/egusphere-2023-2666
Preprint. Discussion started: 15 November 2023

Table 2. Table presenting the soil carbon-concentration (β_s, PgC ppm^{-1}) and carbon-climate (γ_s, PgC °C^{-1}) feedback parameters for 2xCO$_2$ and 4xCO$_2$ for the CMIP6 ESMs.

Earth System	2xCO$_2$		4xCO$_2$	
Model	β_s	γ_s	β_s	γ_s
ACCESS-ESM1.5	0.242	-29.2	0.127	-37.3
BCC-CSM2-MR	0.861	-50.5	0.763	-83.1
CanESM5	0.544	-21.4	0.620	-31.8
CESM2	0.175	-7.67	0.183	-15.1
GFDL-ESM4	0.397	-25.0	0.371	-31.4
IPSL-CM6A-LR	0.357	-11.9	0.222	-15.3
MIROC-ES2L	0.684	-49.4	0.630	-63.1
MPI-ESM1-2-LR	0.494	-14.4	0.375	-15.6
NorESM2-LM	0.157	-12.0	0.161	-19.5
UKESM1-0-LL	0.351	-24.7	0.307	-32.7
Ensemble mean	0.426	-24.6	0.376	-34.5
Ensemble std	± 0.213	± 14.2	± 0.212	± 21.3

https://doi.org/10.5194/egusphere-2023-2666
Preprint. Discussion started: 15 November 2023

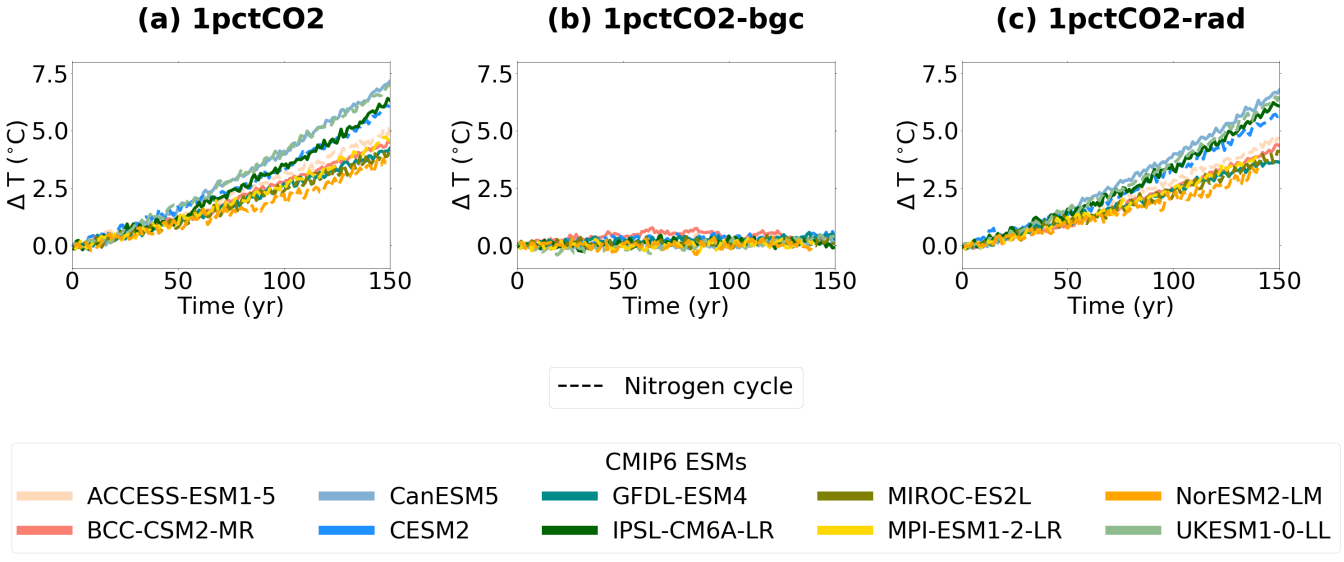

Figure A1. Timeseries of projected global mean temperature changes (ΔT) in CMIP6 ESMs for the idealised simulations 1% CO_2 (left column), biogeochemically coupled 1% CO_2 (BGC, middle column) and radiatively coupled 1% CO_2 (RAD, right column).

https://doi.org/10.5194/egusphere-2023-2666
Preprint. Discussion started: 15 November 2023

Table A1. Table presenting the land carbon-concentration (β_L, PgC ppm^{-1}) and carbon-climate (γ_L, PgC °C^{-1}) feedback parameters for 2xCO_2 and 4xCO_2 for the CMIP6 ESMs.

Earth System	2xCO_2		4xCO_2	
Model	β_L	γ_L	β_L	γ_L
ACCESS-ESM1.5	0.624	-64.5	0.312	-77.7
BCC-CSM2-MR	1.63	-62.1	1.39	-98.0
CanESM5	1.34	-21.6	1.27	-36.9
CESM2	0.839	-18.3	0.787	-30.1
GFDL-ESM4	1.00	-42.3	0.891	-57.3
IPSL-CM6A-LR	1.05	-18.4	0.614	-24.5
MIROC-ES2L	1.34	-56.7	1.08	-74.0
MPI-ESM1-2-LR	1.03	-9.81	0.699	-9.98
NorESM2-LM	0.811	-22.2	0.740	-35.3
UKESM1-0-LL	1.00	-35.6	0.746	-52.4
Ensemble mean	1.07	-35.2	0.854	-49.6
Ensemble std	± 0.281	± 19.1	± 0.304	± 26.0